

# Interaction of 1,2,4-substituted piperazines, new serotonin receptor ligands, with 5-HT<sub>1A</sub> and 5-HT<sub>2A</sub> receptors

Zdzisław Chilmonczyk<sup>a,b,\*</sup>, Marcin Cybulski<sup>c</sup>, Joanna Iskra-Jopa<sup>c</sup>,  
Ewa Chojnacka-Wójcik<sup>d</sup>, Ewa Tatarczyńska<sup>d</sup>, Aleksandra Kłodzińska<sup>d</sup>,  
Andrzej Leś<sup>c,e</sup>, Agnieszka Bronowska<sup>e</sup>, Ingebrigt Sylte<sup>f</sup>

<sup>a</sup> Drug Institute, 30/34 Chełmska Str., 00-725 Warsaw, Poland

<sup>b</sup> Institute of Chemistry, University of Białystok, Al. Piłsudskiego 11/4, 15-443 Białystok, Poland

<sup>c</sup> Pharmaceutical Research Institute, 8 Rydygiera St., 01-793 Warsaw, Poland

<sup>d</sup> Institute of Pharmacology Polish Academy of Sciences, 12 Smętna St., 31-343 Cracow, Poland

<sup>e</sup> Department of Chemistry, University of Warsaw, 1 Pasteura St., 02-093 Warsaw, Poland

<sup>f</sup> Department of Pharmacology, Institute of Medical Biology, University of Tromsø, N-9037 Tromsø, Norway

Received 29 September 2001; accepted 12 January 2002

## Abstract

In the present paper, we describe affinities to 5-HT<sub>1A</sub> and 5-HT<sub>2A</sub> receptors of several new 1,2,4-trisubstituted piperazine derivatives. The affinities were compared with those described earlier for 1,4-disubstituted piperazines and the influence of the third (methyl) substituent on the affinity to both receptors is discussed. The difference between two- and three-substituted derivatives was rationalised in terms of molecular modelling of the respective ligand–receptor complexes. Additionally, the functional activity of some 1,2,4-trisubstituted piperazines for 5-HT<sub>1A</sub> receptor was examined in behavioural and biochemical models. The obtained results have shown that some trisubstituted compounds exhibited a higher affinity to 5-HT<sub>2A</sub> receptors than their respective disubstituted analogues (with the affinity to 5-HT<sub>1A</sub> receptors remaining the same or somewhat improving). The molecular dynamics simulations suggested that the presence of the third substituent in the piperazine ring of those compounds may induce stabilising effect on the ligand–receptor complexes. The results of the *in vivo* studies have shown that some of the examined trisubstituted piperazines (**10–13**, **16**, **17**) exhibited properties of postsynaptic 5-HT<sub>1A</sub> partial agonists. Moreover, compounds **13** and **16** exhibited features of 5-HT<sub>1A</sub> presynaptic agonists in *in vitro* test, and compound **16** also in *in vivo* tests. © 2002 Éditions scientifiques et médicales Elsevier SAS. All rights reserved.

**Keywords:** 5-HT<sub>1A</sub> and 5-HT<sub>2A</sub> receptors; Ligands; Affinity; Intrinsic activity; Molecular modelling

## 1. Introduction

Serotonin (5-hydroxytryptamine, 5-HT) receptors of the 1A sub-population (5-HT<sub>1A</sub> receptor) have recently attracted a considerable attention. It is assumed that anxiolytic and antidepressive drugs such as buspirone (**1**), tandospirone (**2**), gepirone (**3**), ipsapirone (**4**), flesinoxan (**5**) or binospirone (**6**) (Fig. 1)—determined as 5-HT<sub>1A</sub> receptor partial agonists—exert their pharmacological activity through serotonin 5-HT<sub>1A</sub> receptors, where they act as partial agonists [1–3]. Therefore, ligands of the 5-HT<sub>1A</sub> receptor may be considered to be

potential anxiolytic and/or antidepressive drugs. The pharmacological data do not allow to estimate the relative contribution of pre- and postsynaptic 5-HT<sub>1A</sub> receptors to their therapeutic action [4]. It has also been suggested that 5-HT<sub>1A</sub> receptor antagonists may have a beneficial effect in anxiety and depression, as demonstrated by a large number of new substances with 5-HT<sub>1A</sub> antagonistic activity as potential anxiolytics/antidepressants reported in Drug Status Update [5].

Most recently, there has been some interest in compounds that act both at 5-HT<sub>1A</sub> and 5-HT<sub>2</sub> receptors as potential therapeutic agents. Compounds with dual activity at these receptor systems were predicted to be more efficacious than those acting at either subtype alone. Such was the case with arylpiperazine

\* Corresponding author.

E-mail address: [chilmon@il.waw.pl](mailto:chilmon@il.waw.pl) (Z. Chilmonczyk).

derivatives—flibanserin (**7**) (BIMT-17, Behringer Ingelheim Corp.) and adatsanserin (**8**) (WY-50324, Wyeth Ayerst International Inc., Fig. 1)—5-HT<sub>1A</sub> agonists with 5-HT<sub>2</sub> antagonistic activity, which showed a robust activity in preclinical models of depression and anxiety [6–8].

In the present paper, we describe the binding profile on 5-HT<sub>1A</sub> and 5-HT<sub>2A</sub> receptors of several new [9] 1,2,4-trisubstituted piperazine derivatives (Table 1). The affinities were compared with those obtained for 1,4-disubstituted piperazines [10,11] and the influence of the third (methyl) substituent on the affinity to both of the receptors was discussed. The difference between two- and three-substituent derivatives was rationalised in terms of molecular dynamics modelling of the respective ligand–receptor complexes. Furthermore, the in-

trinsic activity of some 1,2,4-trisubstituted piperazines for 5-HT<sub>1A</sub> receptor was examined in behavioural and biochemical models.

## 2. Experimental

### 2.1. Binding studies

The affinity of the compounds for central 5-HT<sub>1A</sub> and 5-HT<sub>2A</sub> receptors *in vitro* was assessed on the basis of their ability to displace [<sup>3</sup>H]-8-OH-DPAT and [<sup>3</sup>H]ketanserin, respectively. Radioligand binding studies were performed in the rat brain using the following structures: hippocampus (5-HT<sub>1A</sub>) and cortex (5-HT<sub>2A</sub>) according to the published procedures [12,13].

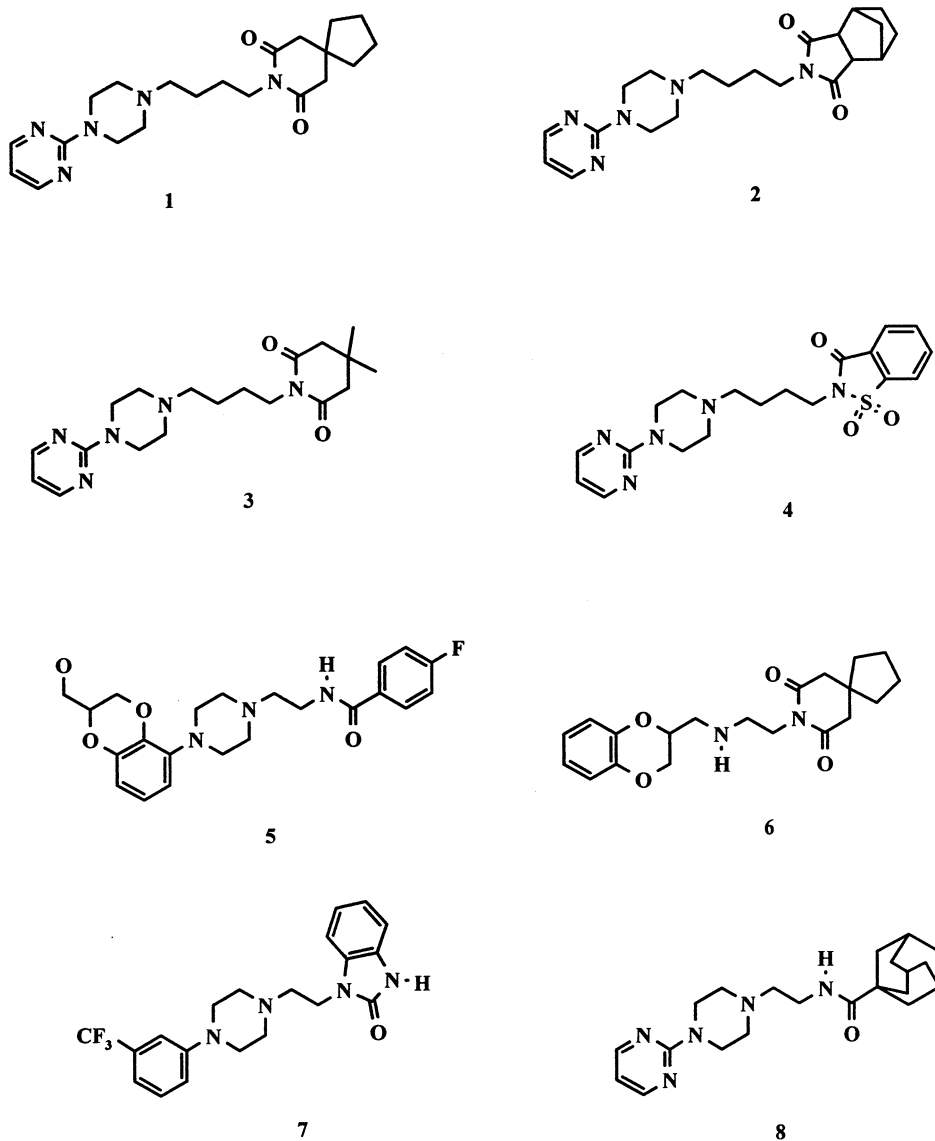
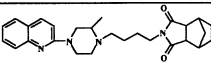
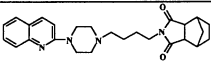
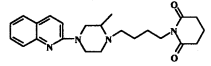
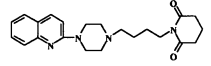
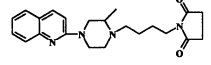
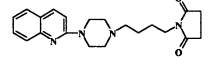
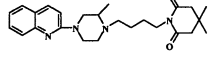
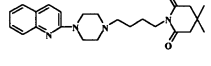
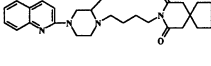
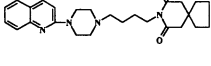
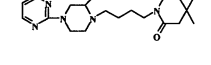
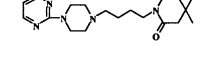
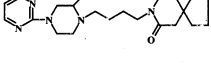
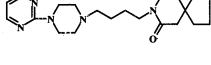
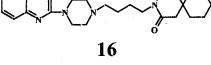
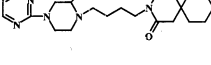


Fig. 1. Chemical structures of buspirone (**1**), tandospirone (**2**), gepirone (**3**), ipsapirone (**4**), flesinoxan (**5**), binsospirone (**6**), flibanserin (**7**) and adatsanserin (**8**). P. 41.

Table 1  
5-HT<sub>1A</sub> and 5-HT<sub>2A</sub> receptors affinities ( $K_i \pm \text{SEM}$  [nM]) of compounds **1**, **3**, **9–22**

Trisubstituted piperazines			disubstituted piperazines		
Compound	5-HT <sub>1A</sub>	5-HT <sub>2A</sub>	Compound	5-HT <sub>1A</sub>	5-HT <sub>2A</sub>
ritanserin*	---	1.12±0.04			
 <b>9</b>	26±2	18±8	 <b>18</b>	29±4 <sup>^</sup>	580±138 <sup>^</sup>
 <b>10</b>	37±6	185±23	 <b>19</b>	48±3 <sup>^</sup>	294±6 <sup>^</sup>
 <b>11</b>	107±46	122±29	 <b>20</b>	83±2 <sup>^</sup>	51716 <sup>^</sup>
 <b>12</b>	15±3	64±26	 <b>mesmar (21)</b>	11±2 <sup>^^</sup>	107±20 <sup>^</sup>
 <b>13</b>	24±3	32±3	 <b>kaspar (22)</b>	39±7 <sup>^^</sup>	3442±961 <sup>^</sup>
 <b>14</b>	493±52	6044±237	 <b>gepirone (3)</b>	32 <sup>∅</sup>	3630 <sup>⊕</sup>
 <b>15</b>	167±31	1240±384	 <b>buspirone (1)*</b>	14±2 <sup>^</sup>	794 <sup>⊕</sup>
 <b>16</b>	13±1	108±16	 <b>17</b>	29±8	1306±153

\*Reference compounds; <sup>^</sup>, ref. [11]; <sup>^^</sup>, ref. [10]; <sup>∅</sup>, ref. [66]; <sup>⊕</sup>, ref. [67]; <sup>⊙</sup>, ref. [68].

Buspirone and ritanserin were employed as reference compounds. Radioligands used were [<sup>3</sup>H]-8OH-DPAT (190 Ci/mmol, Amersham) and [<sup>3</sup>H]ketanserin (60 Ci/mmol, NEN Chemicals) for 5-HT<sub>1A</sub> and 5-HT<sub>2A</sub>, respectively.  $K_i$  values were determined from three competition binding experiments in which several drug concentrations run in triplicates were used.

## 2.2. In vivo experiments

The activity of the compounds was evaluated on male Wistar rats (250–280 g) or on male Albino-Swiss

mice (26–29 g). The animals were kept at a room temperature of  $21 \pm 1$  °C on a natural day–night cycle; they were housed in plastic boxes (55 × 35 × 20 cm) in the groups of eight (rats) or 30 (mice) animals, with free access to food (Bacutil pellets) and tap water throughout the experiment. Experimental and control groups consisted of six to eight animals each. The tested compounds were administered as suspensions in a 1% aqueous solution of Tween 80, 8-OH-DPAT, reserpine and (*S*)-WAY 100135 as solutions in physiological saline. Tested compounds were administered intraperitoneally (i.p.), and 8-OH-DPAT, reserpine and (*S*)-

WAY 100135 subcutaneously (s.c.) in a volume of four (rat) and ten (mouse) ml/kg. The control groups of animals received the same amounts of the solvent. Newman–Keuels test was used for the statistical evaluation. 8-Hydroxy-2-(di-*n*-propylamino)tetralin hydrobromide (8-OH-DPAT·HBr) was purchased from RBI, (*S*)-*N*-*tert*-butyl-3-[4-(2-methoxyphenyl)piperazin-1-yl]-2-phenylpropanamide ((*S*)-WAY-100135) was synthesised by Dr. J. Boksa, Institute of Pharmacology, Polish Academy of Sciences, and reserpine in ampoules was purchased from Ciba–Geigy.

### 2.3. Lower lip retraction (LLR) in rats

The LLR was conducted according to the method described by Berendsen et al. [14]. The animals were individually placed in cages, having been scored three times at 15, 30 and 45 min (each observation time—45 s) after administration of tested compounds or 8-OH-DPAT as follows: 0 = lower incisors invisible, 0.5—partly visible, 1—clearly visible. The summed up, maximum score was up to 3 for each rat. In a separate experiment, the effect of tested compounds or (*S*)-WAY-100135 on 8-OH-DPAT (1 mg/kg)-induced LLR was tested. The tested compounds were administered 45 min before 8-OH-DPAT. The observation session started 15 min after the injection of 8-OH-DPAT and were repeated at 30 and 45 min.

### 2.4. Behavioural syndrome in reserpinised rats

Reserpine (1 mg/kg) was administered 18 h before tests. The animals were individually placed in cages 5 min before injection of tested compounds or 8-OH-DPAT. Observation sessions, lasting 45 s each, began 3 min after drug administration and were repeated every 3 min over the period of 15 min. Flat body posture and reciprocal forepaw treading were scored using a ranked intensity scale: 0 = absent, 1 = equivocal, 2 = present, 3 = intense, according to Tricklebank et al. [15]. The maximum score, summed up over five observation periods, amounted to 15 for each symptom per animal. In a separate experiment, the effect of tested compounds or (*S*)-WAY 100135 on the 8-OH-DPAT (5 mg/kg)-induced behavioural syndrome was tested. The tested compounds were administered 45 min before 8-OH-DPAT and animals were scored 3, 6, 9, 12, and 15 min after the injection of 8-OH-DPAT.

### 2.5. Body temperature in mice

The rectal body temperature of mice (2.5 cm deep, Ellab thermometer, Denmark) was recorded at 30, 60, 90 and 120 min after the injection of a tested compounds or 8-OH-DPAT.

In a separate experiment, the effect of compounds **10**,

**12**, **17** or (*S*)-WAY-100135 on 8-OH-DPAT (5 mg/kg)-induced hypothermia was tested. The compounds were administered 45 min before 8-OH-DPAT. The observation sessions started 15 min after the injection of 8-OH-DPAT and were repeated at 30, 45 and 60 min.

In another experiment, the effect of (*S*)-WAY 100135 (10 mg/kg) on the hypothermia induced by compounds **9**, **10**, **11**, **13** and **16** was investigated. (*S*)-WAY 100135 was administered 30 min before the tested compounds. The rectal body temperature was measured 30 min after their injection.

The results were expressed as a change in the body temperature ( $\Delta t$ ) with respect to the basal body temperature, as measured at the beginning of the experiments (the mean value out of two measurements).

### 2.6. Biochemical estimations

5-HT and 5-HIAA contents in the frozen tissue samples were measured by HPLC–EC according to the procedure described elsewhere [16,17]. Male Wistar rats (230–270 g) were housed under artificial light/dark conditions (the light on from 07:00–19:00 h) and fed on a standard granulated diet (Bacutil) with free access to tap water; the ambient temperature was 22 °C. In the biochemical study compounds **13** and **16** were injected intraperitoneally (i.p.) in a single dose of 30 mg/kg in the form of 1% suspension in Tween 80 (1 ml per rat) and 8-OH DPAT was administered i.p. in dose 5 mg/kg in 1% Tween 80 (300  $\mu$ l per rat). The rats were killed by decapitation for biochemical assays 60 min after an i.p. injection of compounds: **13** and **16** and 30 min after an i.p. injection of 8-OH DPAT. The brains were dissected into two regions (hippocampus and striatum) on an ice-plate and stored under solid CO<sub>2</sub>. The tissue samples were weighed and homogenised (1:10 wet wt./vol) in ice cold 0.1 M trichloroacetic acid containing 0.05 mM ascorbic acid. After centrifugation (4000 rpm, 4 °C, 20 min), supernatants were filtered off through durapore Millex-HV 0.22  $\mu$ m membranes (Millipore). 5-HT and 5-HIAA levels were determined by HPLC with electrochemical detection. A Waters™ 616 liquid chromatograph with Waters 464 electrochemical detector was equipped with Waters Spherisorb 10  $\times$  4.6 mm guard cartridge and 5  $\mu$ m Waters Spherisorb ODS2 250  $\times$  4.6 mm column. The mobile phase consisted of 31.2 g NaH<sub>2</sub>PO<sub>4</sub>, 0.32 g heptanesulfonic acid, 0.6 g EDTA, 130 ml CH<sub>3</sub>CN, water up to 2 l adjusted to pH 2.88 with 3 M H<sub>3</sub>PO<sub>4</sub>. The flow rate was maintained at 1 ml/min. The applied voltage was set at 0.60 V versus Ag/AgCl electrode. The compounds were quantified by peak height comparison with standard run on day of analysis, with a sensitivity of 3–100 pg.

The statistical significance was calculated using *t*-test (STATISTICA, StatSoft).

Results are means with SEM of data obtained from five animals per group.

## 2.7. Molecular modelling

### 2.7.1. Ligands preparation

The starting structures of **13** and **15** were prepared based on the crystal structure of 4,4-dimethyl-1-{4-[2-quinolinyl]-1-piperazinyl}butyl}-2,6-piperidinedione [10]. The methyl group was attached to the piperazine ring using AMBER 5.0 [21] and MIDASPLUS software [18]. The nitrogen atom of piperazine ring bound to the *n*-butyl moiety was considered as protonated in both cases. After an initial energy minimisation the restrained electrostatic potential fitted charges (RESPs) [19] were calculated using an RHF/6-31G\* basis set, using GAUSSIAN94 program [20]. The RESP charges were used in a further geometry optimisation, until convergence with a 0.002 kcal/mol Å energy gradient difference between successive steps. The next step was an iterative procedure, where a new set of RESP charges was generated and used in the subsequent energy minimisation. Afterwards, the set of conformers for each ligand was generated by the Molecular Dy-

namics (MD) 750 ps simulation: after an initial equilibrium period at 0.1 K, the MD simulations with velocity scaling were performed at 310 K, with the step-length 0.001 ps. Potentially bioactive conformers, i.e. such conformers that fitted the biophore models for 5-HT<sub>1A</sub> and 5-HT<sub>2A</sub> (Fig. 2) [22] were selected, in a manner described in detail elsewhere [22,23]: each conformer with a deviation within 1.15 Å in atomic distance between the selected atoms corresponding to the biophore model was energy minimised and the lowest-energy conformers were selected afterwards.

In the present work all molecular mechanic energy minimisations and MD simulations were performed by AMBER 5.0 [21] with the AMBER all-atom force field. In order to include the solvent effects a distance-dependent dielectric function ( $\epsilon = 4r$ , where  $r$  is the interatomic distance) without explicit molecules of a solvent was used in the calculations [24,25].

### 2.7.2. Receptor modelling

The 3-D 5-HT<sub>1A</sub> receptor model was constructed from the amino acid sequence of the human 5-HT<sub>1A</sub> receptor [26]. An initial model of the transmembrane helical (TMH) bundle was constructed by analogy to the previous 5-HT<sub>1A</sub> receptor model [27]. Minor changes in tilting and the axial rotations of some TMHs are further described elsewhere [22]. Because the receptor construction was performed before the crystal structure of rhodopsin was published [28], the TMHs were organised according to the projection map of visual rhodopsin [29,30] using the TMHs arrangement of G protein-coupled receptors proposed by Baldwin [31,32], see Fig. 3. Loops end termini were energy-minimised and then connected to the TMHs. The N-terminus was directly copied from the previous 5-HT<sub>1A</sub> receptor model [27], energy-minimised and then connected to the TMH1. Initial structures of the remaining extramembranous segments, except for ICL3, were constructed by searching for loop segments in the Brookhaven PDB-database. The criteria used for the selection of these fragments were: the maximal sequence similarity and the lowest energy. The intracellular loop (ICL3) consists of 133 amino acids, far too many to apply the sequence homology described above. Thus, the structure of this fragment was generated by using the Predict-Protein server ([http://www.embl.columbia.edu/pp/submit\\_adv.html](http://www.embl.columbia.edu/pp/submit_adv.html)). The conformation of  $\alpha$ -helix was predicted for residues 4–11 and 93–111, while the  $\beta$ -sheet structure was predicted for residues 37–44 and 61–73. For the remaining part of the sequence, predicted in a random conformation, the same strategy as for the other loops was applied, with the same criteria used. The PDB identification codes for the sequence fragments used as initial structure of extramembranous domains and the further details are shown elsewhere [22,23].

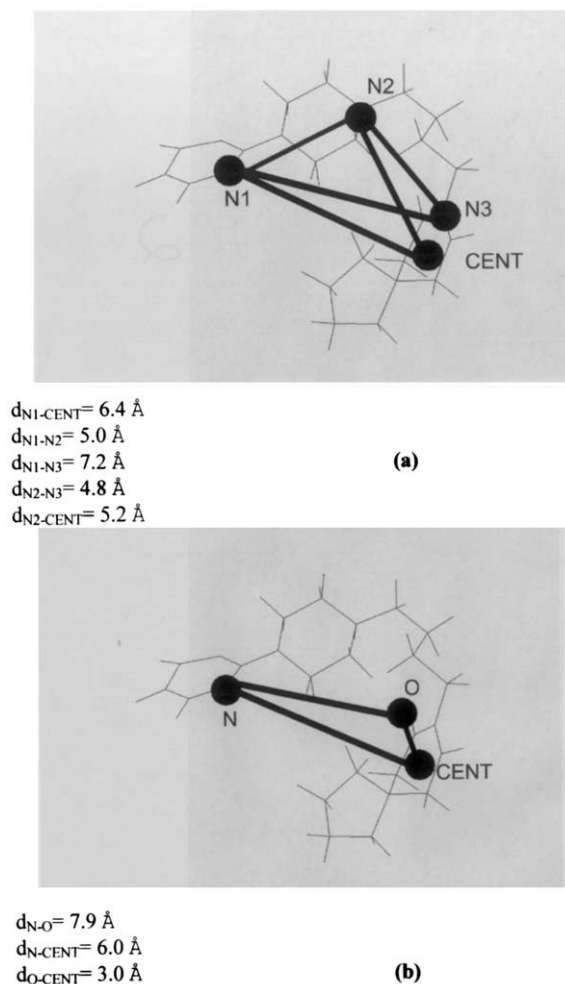


Fig. 2. Biophore models for 5-HT<sub>1A</sub> (a) and 5-HT<sub>2A</sub> (b) receptors. The biophore elements (N1, N2, N3, O, CENT) are marked on the buspirone molecular structure. P. 42.

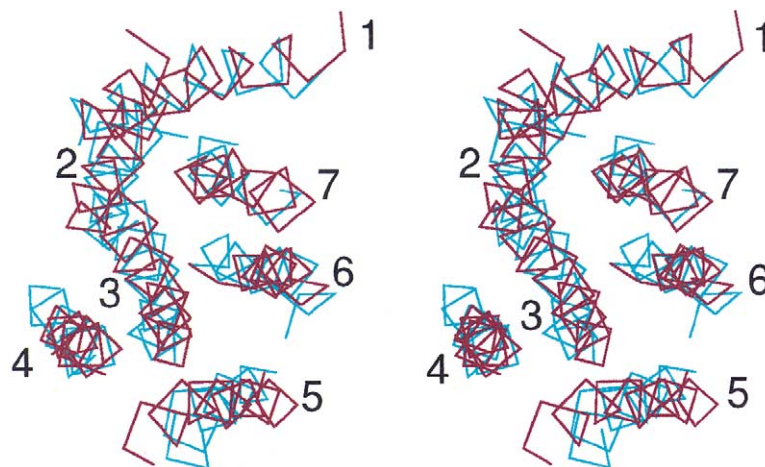


Fig. 3. Superimposed seven TMH bundle of 5-HT<sub>1A</sub> receptor model (blue) and rhodopsin (red) crystal structure, viewed from the extracellular side. P. 43.

The structure of receptor model was afterwards energy-refined in the course of 25 ps MD simulation of the loops and termini, first while keeping the helices at a fixed position, then by energy minimisation of the entire receptor model. A disulfide bridge between conserved cysteine residues C3.25(C109) and C187 in ECL2, known to form an important structural constraint in many GPCRs [25], was present during all simulations.

By analogy, the 5-HT<sub>2A</sub> receptor model was constructed from the sequence of the human 5-HT<sub>2A</sub> receptor [33], with the similar conditions as the 5-HT<sub>1A</sub> TMHs and the intra- and extracellular loops (ICLS and ECLs) except for ICL3 and ECL2 of the 5-HT<sub>1A</sub> receptor, were used as a template in constructing of 5-HT<sub>2A</sub> receptor. The ICL3, ECL2 and the termini were constructed by the sequence homology and added afterwards. The entire model was finally energy minimised.

Such receptor models were used afterwards as starting structures for the 30 ps MD simulation, while the temperature were increased from 0 to 300 K, 50 K per each 5 ps of simulation. The further 140 ps of MD simulation was performed while keeping the temperature at 300 K.

To preserve the helical conformations of TMHs the constraints forces of the 5 kcal/mol Å<sup>2</sup> were used [34], applied between the backbone oxygen atom of residue *n* and the backbone nitrogen atom of residues *n* + 4, excluding prolines. Initial simulations indicated that such interhelical constraint forces were important to produce rigid body helical movements as observed in experimental studies [35,36]. A similar strategy to constraining helices, together with distance-dependent dielectric function and dielectric constant  $\epsilon = 4r$ , has also been used previously during MD simulations of G protein-coupled receptors [37,38].

The 30 coordinate sets saved between 140 and 170 ps were used to calculate the average structures of receptor models, which finally were energy-refined.

### 2.7.3. Ligand–receptor interactions

In order to start the docking procedure, potentially bioactive conformers of **13** and **15** were docked into a central cavity of 5-HT<sub>1A</sub> and 5-HT<sub>2A</sub> receptor models, using the data obtained from site-directed mutagenesis experiments [26,39–54] as a guide. Each conformer was docked in two different positions, in which the protonated amino group of the piperazine ring were placed close to the conserved aspartic acid (Asp116 in 5-HT<sub>1A</sub> or Asp155 in 5-HT<sub>2A</sub>, respectively) in TMH3. Four ligand–receptor complexes were energy minimised afterwards and such complexes (two per receptor, involving one conformer of ligand docked in two different positions) that create the best ligand–receptor fit were selected for further calculations.

The selected ligand–receptor complexes were used as initial structures for short (30 ps) molecular dynamics simulation. In parallel, such simulations were performed for the ligand-unbound receptor structures. The coordinate sets obtained after those 30 ps of MD simulation were saved and used as initial structures for further 140 ps MD simulation at constant temperature and using constraint forces to preserve a TMH helical conformation, as for the isolated receptor described above. The 30 coordinate sets saved between 140 and 170 ps were used to calculate the average structures of ligand–receptor complexes, which were energy-minimised afterwards. At last, two positions of ligands were compared and the complex (one per ligand) creating better ligand–receptor fit was selected for further investigations.

### 3. Results and discussion

The receptor affinities of the investigated compounds **9–17** (hydrochlorides) were determined in competition-experiments using 8-hydroxy-2-di-*n*-propylaminotetra-line ( $[^3\text{H}]$ -8-OH-DPAT) for 5-HT<sub>1A</sub> and  $[^3\text{H}]$ ketanserin for 5-HT<sub>2A</sub> receptors (Table 1).

It appeared that **6** out of **9** new 1,2,4-trisubstituted piperazines exhibited a significant affinity ( $K_i < 100$  nM) to 5-HT<sub>1A</sub> receptors. Compounds **12** and **16** possessed the highest ( $K_i = 15 \pm 3$  and  $13 \pm 1$  nM, respectively) and compound **14** the lowest ( $K_i = 493 \pm 52$  nM) affinity. Only compounds **9**, **12** and **13** exhibited a relatively high affinity to 5-HT<sub>2A</sub> receptors ( $K_i = 18 \pm 8$ ,  $64 \pm 26$  and  $32 \pm 3$  nM, respectively). The affinity of the other compounds to 5-HT<sub>2A</sub> receptors was low or very low. Compound **12** possessed a high affinity to both of the receptors. It should be noted that trisubstituted piperazine-quinoline derivatives (compounds **9**, **10**, **11**, **12**, **13**) exhibited a much higher affinity to 5-HT<sub>2A</sub> receptors than the respective disubstituted compounds (**18**, **19**, **20**, mesmar (**21**), kaspar (**22**) [10,11]. At the same time the affinity of the respective (trisubstituted against disubstituted piperazine-quinolines) compounds to 5-HT<sub>1A</sub> receptors almost does not change. On the other hand, trisubstituted piperazine-pyrimidine derivatives (compounds **14** and **15**) possessed a much lower affinity to both of the receptors than their disubstituted analogues (compounds **1** and **3**). The results thus show that the presence of the third substituent (methyl group) in the piperazine ring is beneficial in the series of quinoline derivatives (compounds **9**, **10**, **11**, **12**, **13** and **16**), but not in the series of pyrimidine derivatives **14**, **15** and **17**. Trisubstituted piperazine-quinolines exhibited affinity to 5-HT<sub>1A</sub> and 5-HT<sub>2A</sub> receptors much higher than their pyrimidine analogues (compounds **12**, **13** and **16** against compounds **14**, **15** and **17**, respectively). Such a difference in the affinities of quinoline and pyrimidine derivatives could be explained in terms of unique 3-D structures formed by the respective ligand–receptor complexes. For this reason four complexes were examined, i.e. two of the pyrimidine derivative **15**-5-HT<sub>1A/2A</sub> and another two of the quinoline derivative **13**-5-HT<sub>1A/2A</sub> (Fig. 4: **13**-5-HT<sub>1A</sub>, **15**-5-HT<sub>1A</sub> and Fig. 5: **13**-5-HT<sub>2A</sub>, **15**-5-HT<sub>2A</sub>).

#### 3.1. Modelling of the ligand–receptor interactions

In the present study some aspects of ligand–receptor interactions such as the ligand position inside the receptor cavity, receptor 3-D structure modification upon the ligand binding (translation of helices, conformational changes of intracellular loops or movements of certain sequence motifs), and identification of amino acids important for ligand binding were examined. The calculations were initially based on the available site-directed

mutagenesis data identifying amino acids, TMHs and loops crucial for ligand binding and receptor activation [26,39–52]. These data, obtained for selected GPCRs, were used as a guide for ligand docking. These results allowed for reduce significantly the number of potential sites of ligand docking. These data allowed for a more rationalised docking procedure that should lead to find the most realistic binding site. However, it is recommended to further test the ligand binding modes by site-directed mutagenesis studies, which may verify the validity of the present methodology and obtained models.

A qualitative comparison between obtained models of ligand-unbound serotonin receptors and the crystallographic structure of rhodopsin, Fig. 3, suggests the usefulness and validity of the present receptor models, although the helical bundles of these receptors were constructed using the projection map of rhodopsin as a guide and not its crystal structure. It happened, because the present results were obtained before the crystal structure of visual rhodopsin was published [28]. Despite that, the overall helical packing and the orientation of the helices relative to each other of obtained ligand-unbound 5-HT<sub>1A</sub> and 5-HT<sub>2A</sub> receptor models were found in very good accordance with rhodopsin X-ray structure, as shown in Fig. 3. In both serotonin receptor models, the orientations of particular amino acid residues, which are highly conserved among the family A of GPCRs, were found at positions similar to those of the rhodopsin structure. However, the conformation of both receptors binding the compound (**13**) differed significantly from the crystal structure of rhodopsin. The helical rigid body movements, together with rotational changes and different tilting of the particular helices contributed mainly to these alterations. Also, orientations of many highly conserved amino acid residues changed upon the ligand binding. More details are described elsewhere [22,23,25]. It is known that crystal structure of rhodopsin correspond to rhodopsin in its inactive state [28]. Therefore, observed differences between ligand–receptor complex and X-ray structure of rhodopsin seem to reflect the receptor activation induced by the binding of the ligand.

#### 3.2. 5-HT<sub>1A</sub> receptor

In **13**-5-HT<sub>1A</sub> and **15**-5-HT<sub>1A</sub> complexes after molecular dynamics (MD) simulations close contacts between the ligands and certain receptor amino acid residues were observed. Such close contacts may be interpreted as ligand–receptor interactions and concerned all moieties (i.e. aromatic, methylated piperazine, *n*-butyl, and imide) of both investigated analogues. The most important ligand–receptor contacts can be described as follows: compound **13** interacted with amino acid residues

in TMH1 (Leu46 being the only contact found), TMH2 (Val89 and Met92), TMH3 (Cys109, Phe112, Asp116, Cys120, and Ser123), TMH4 (Gly174 and Trp175), TMH5 (Thr196, Ile197, and Thr200), TMH6 (Trp358, Phe361, and Ala365), and TMH7 (Ile385, Tyr390, Ser393); compound **15** interacted with residues in TMH2 (Leu88, Val89, and Met92), TMH3 (Phe112, Asp116, Val117, Cys120), TMH5 (Ile197 and Tyr198), TMH6 (Trp358, Phe361, Phe362, Leu366), and TMH7 (Asn386, Tyr390, Ser393) (Table 2, Fig. 4).

During MD simulation ligand-induced changes of the receptor 3-D structure were observed. The rigid body movements of TMH 2, 3, 6, and 7, associated with the rearrangement of the receptor interhelical hydrogen bonding network were observed in the **13**-receptor complex as compared with the free receptor structure (the strongest displacement was found for TMH3 and 6). Compound **15** caused the movements of TMHs 3, 6, and 7, however, these movements were weaker than those induced by compound (**13**). During

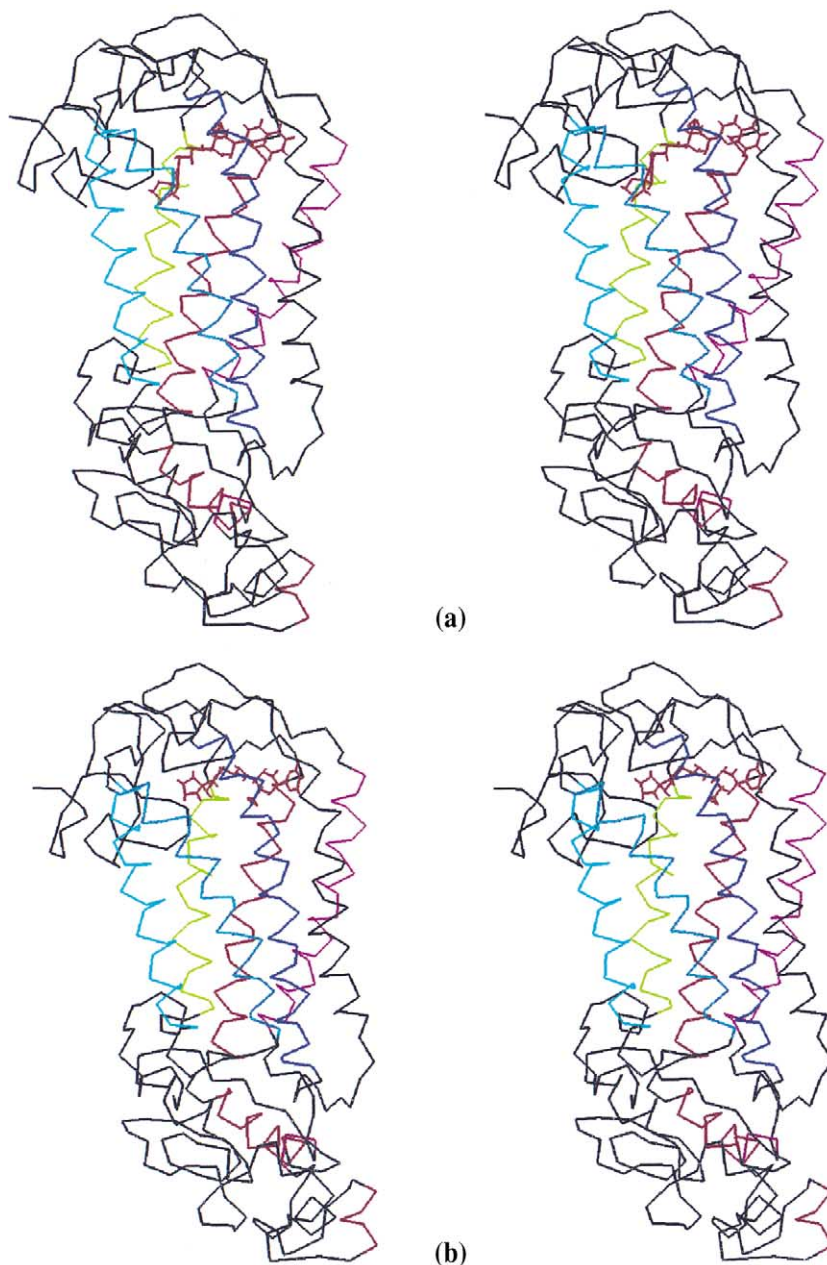


Fig. 4. Stereo view of average, energy-minimised **13**-5-HT<sub>1A</sub> (a) and **15**-5-HT<sub>1A</sub> (b) complexes. View along the plane of membrane, perpendicularly to the long axis of the receptor. The ligand is coloured blue. The methyl group of the ligand, substituted in piperazine ring, is marked by the triangle. Seven TMHs of receptors are specified by colours: TMH1—dark blue, TMH2—orange, TMH3—cyan, TMH4—black, TMH5—green, TMH6—yellow and TMH7—red. The N-terminus and ECLs are at the top of the panel, while ICLs and the C-terminus are at the bottom of the panel (below the TMHs). P. 44



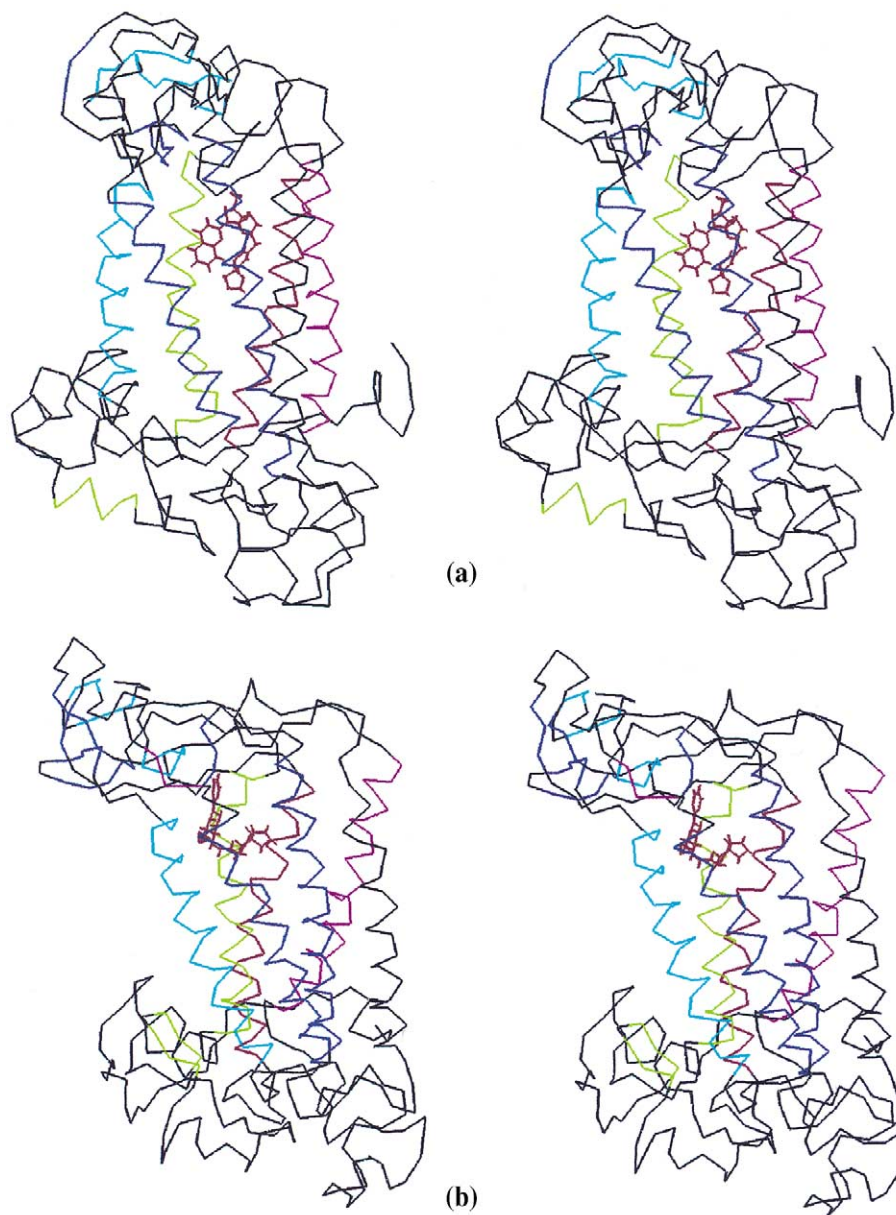


Fig. 5. Structures of average, energy-minimised **13**-5-HT<sub>2A</sub> (a) and **15**-5-HT<sub>2A</sub> (b) complexes. Ligands and TMHs of the receptor are coloured and viewed as in Fig. 4. P. 45.

these displacements some differences in tilting were observed for TMH6, while tilting of TMH3 became practically unchanged. While interacting with (**13**), TMHs 4 and 5 changed its rotational orientation, and tilting of TMHs 2, 5 and 7 was slightly altered, as well. These conformational changes of the receptor structure induced by **13** are illustrated in Fig. 6. Rigid body movements of TMHs have been observed previously in the process of rhodopsin photoactivation [43]. Helical rigid body movement has also been suggested in the activation mechanism of the muscarinic M2 receptor [36]. Results of experiments performed on the  $\beta_2$ -adrenoreceptor have also suggested that agonist induced conformational changes and displacements of

TMHs: 3 and 6 are crucial for receptor activation [47].

It should be noted that quinoline derivative **13** induced (to higher extent than pyrimidine derivative **15**) such conformational changes in second and third intracellular loops (the approaching of the loops) that might be important for a G-protein binding [51]. Compound **13** also induced the repositioning of the highly conserved in G-protein coupled receptors D-R-Y amino acid sequence motif in TMH3 which was suggested as a crucial for a receptor activation [48,51].

Taken together, the above MD simulation data showed that the conformations and positions of compounds **13** and **15** inside the 5-HT<sub>1A</sub> receptor were significantly different. They also showed that

compound **13** induced greater conformational changes in the receptor, particularly in the regions suggested by site-directed mutagenesis data as important for ligand binding and receptor activation. Thus, the above theoretical results suggest that compound **13** should exhibit a higher affinity to the receptor than compound **15**. They also suggest that compound **13** (5-HT<sub>1A</sub> receptor

Table 2

Residues lying within 20% increased van der Waals radii around compounds **15** and **13** in their respective ligand-5-HT<sub>1A</sub> and ligand-5-HT<sub>2A</sub> receptor complexes

Ligand <sup>a</sup>	Aromatic moiety	Piperazine ring	<i>n</i> -Butyl moiety	Imide moiety
<i>5-HT<sub>1A</sub></i>				
<b>13</b>	Gly174(4) His193(5) Gly194(5) Thr196(5) Ile197(5) Ala365(6) Pro369(6) Ile385(7)	Ile113(3) Asp116(3) Val117(3) Phe361(6) Ala365(6) Ile385(7)	Asp116(3) Val117(3) Cys120(3) Trp358(6) Phe361(6) Gly389(7)	Leu46(1) Val89(2) Met92(2) Asn386(7) Gly389(7) Tyr390(7) Ser393(7) Ala186(E2) Cys187(E2)
<b>15</b>	Ile113(3) Thr188(E2) Ile197(5) Leu366(6) Pro369(6) Leu381(7)	Val117(3) Cys120(3) Phe362(6) Ala365(6) Ile385(7) Asp116(3) Thr188(E2),	Trp358(6) Phe361(6) Gly389(7)	Val85(2) Leu88(2) Val89(2) Met92(2) Phe112(3) Asp116(3) Asn386(7) Gly389(7) Tyr390(7) Ser393(7)
<i>5-HT<sub>2A</sub></i>				
<b>13</b>	Leu123(2) Asp155(3) Val156(3) Phe158(3) Ser159(3) Ser162(3) Phe364(7) Ile367(7) Gly368(7) Ser371(7)	Ala359 (7) Val363(7) Phe364(7) Asp155(3)	Phe243(5) Cys336(6) Glu339(6) Ile340(6) Ile343(6)	Ile163(3) Phe243(5) Trp335(6) Cys336(6) Ser371(7) Val374(7)
<b>15</b>	Val47(NT) Asp48(NT) Ser49(NT) Asn54(NT) Leu360(7) Leu361(7) Phe364(7)	Trp76(1) Ser77(1) Leu80(1) Thr81(1) Val84(1) Asp155(3) Ile367(7) Gly368(7)	Thr81(1) Val84(1) Leu123(2) Ser371(7)	Gly124(2) Leu126(2) Val127(2) Val130(2) Ser131(2) Val150(3) Trp151(3) Leu154(3) Asp155(3) Phe158(3)

Results of molecular modelling simulations.

<sup>a</sup> Four fragments of the ligand, i.e. aromatic moiety, piperazine ring, butyl moiety and imide moiety, are treated separately due to a better description of the binding site topography. Location of a residue in the TMH domain (X), ECL (EX) or N-terminus (NT) is given in brackets.

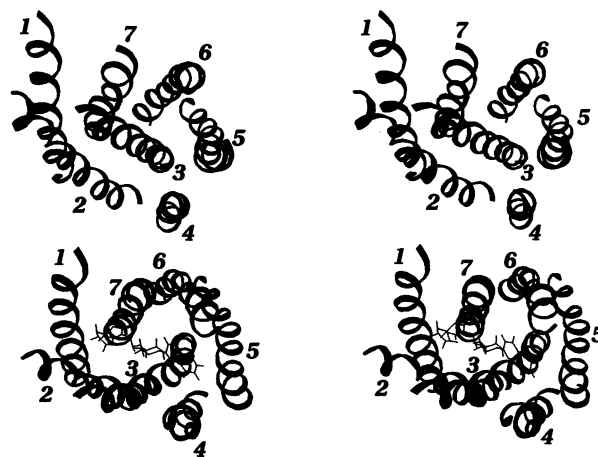


Fig. 6. Stereo view of average, energy-minimised 5-HT<sub>1A</sub> free receptor (upper panel) and the **13**-5-HT<sub>1A</sub> complex (lower panel). View from the extracellular side of the membrane, perpendicularly to the long axis of the receptor. TMHs are represented as ribbons and numbered. Positions of TMHs: 1 and 2 have been kept the same, to show the conformational changes and displacements of the other TMHs upon the ligand binding. P. 46.

functional partial agonist) could induce such conformational changes in the receptor structure that could lead to trigger G-protein coupling and the receptor activation.

### 3.3. 5-HT<sub>2A</sub> receptor

In ligand-5-HT<sub>2A</sub> receptor complex the compound **13** interacted with amino acid residues in TMH2 (Leu123 being the only contact found), TMH3 (Asp155, Phe158, Ser159, Ser162), TMH5 (Phe243), TMH6 (Trp335, Cys336, Glu339), and TMH7 (Phe364, Gly368, Ser371, Val374). The compound **15** interacted with residues in TMH1 (Trp76, Ser77, Thr81, Val84), TMH2 (Leu123, Leu126, Val130, Ser131), TMH3 (Val150, Trp151, Asp155, Phe158), TMH7 (Leu361, Ile367, Ser371), and N-terminal (Val47, Asp48, Ser49, Asn54) (Table 2, Fig. 5). It should be noted that significant structural differences between **15**-5-HT<sub>2A</sub> and **13**-5-HT<sub>2A</sub> complexes were observed. Compound **13** induced a strong displacement of the TMHs 2, 3, 6, and 7 (Fig. 7), while compound **15** hardly caused any displacements of TMHs. Additionally, compound **15** (but not **13**) exhibited interactions with those receptor domains (TMH1, N-terminal), that were suggested by site-directed mutagenesis to be unimportant for a ligand binding [42,43,51].

The present modelling results therefore suggest, that the combination of quinoline aromatic moiety and methylated piperazine ring (compound **13**) improved the ligand–receptor adjustment as compared with the combination of pyrimidine aromatic moiety and methylated piperazine ring (compound **15**), the result being consistent with the affinity data.

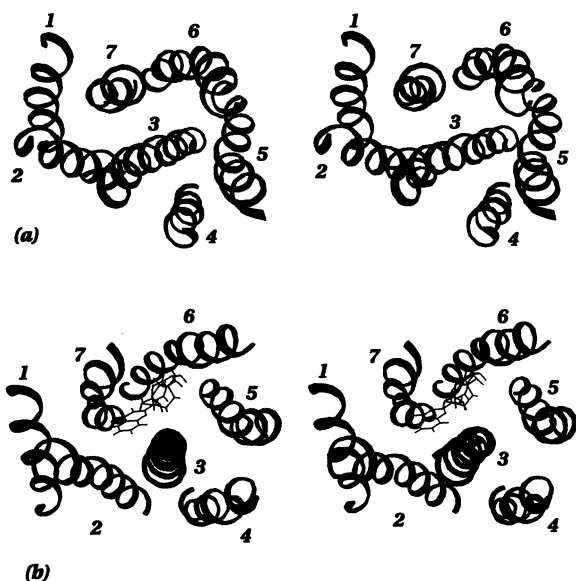


Fig. 7. Structures of average, energy-minimised TMH bundle of 5-HT<sub>2A</sub> free receptor (a) and the 13-5-HT<sub>2A</sub> complex (b), viewed as in Fig. 6. Positions of TMHs: 1 and 2 have been kept the same, to show the conformational changes and displacements of the remaining part of TMH bundle upon the ligand binding. P. 47.

Table 3  
The induction of LLR (A) by compounds 9–13, 16, 17 and their influence on the 8-OH-DPAT (1 mg/kg)-induced LLR (B) in rats

Compound	Dose (mg/kg)	LLR score (mean ± SEM)		
		A <sup>a</sup>	B <sup>b</sup>	
(S)-WAY 100135	2.5	0	2.4 ± 0.4	
	5	0	1.8 ± 0.2 #	
	10	0	0.6 ± 0.2 #	
9	10	0.3 ± 0.1	2.3 ± 0.2	
	20	0.6 ± 0.2	2.2 ± 0.2	
10	5	0.1 ± 0.0	2.4 ± 0.2	
	10	0.5 ± 0.2	2.8 ± 0.1	
	20	0.5 ± 0.3	1.6 ± 0.3 #	
11	5	0.3 ± 0.2	1.7 ± 0.2	
	10	0.3 ± 0.2	1.3 ± 0.1 #	
	20	0.8 ± 0.1*	1.2 ± 0.2 #	
12	10	0.7 ± 0.2	2.3 ± 0.3	
	20	1.4 ± 0.2*	1.3 ± 0.4 #	
	13	5	0.3 ± 0.2	2.4 ± 0.2
13	10	0.2 ± 0.1	2.5 ± 0.2	
	20	2.0 ± 0.3*	NT	
	16	10	0.0 ± 0.0	2.3 ± 0.2
16	20	0.6 ± 0.1	2.2 ± 0.2	
	17	5	0.6 ± 0.2	2.2 ± 0.2
	10	1.1 ± 0.3*	2.0 ± 0.2	
17	20	2.1 ± 0.2*	NT	

\*,  $P < 0.01$  versus vehicle; #,  $P < 0.01$  versus 8-OH-DPAT; NT-not tested.

<sup>a</sup> The respective score for vehicle treated groups was  $0.1 \pm 0.1$ .

<sup>b</sup> The respective score for 8-OH-DPAT treated groups (except for (S)-WAY 100135 where it was  $-3.0 \pm 0.0^*$ ) was  $2.8 \pm 0.1^*$ .

The present results were also compared with those obtained for buspirone (1) and kaspar (22) [22,27]. This comparison suggested that the combination of quinoline (but not pyrimidine) aromatic moiety and methylated piperazine ring should improve the ligand–receptors adjustment as compared with the non-methylated piperazine ring, probably due to different positions adopted by the methylated pyrimidinyl and quinolinyl derivatives. Methylation of compounds possessing an aromatic pyrimidinyl ring induces strong, improper constraints into the structural/dynamical complementarity between the ligand and the receptor, altering the ligand position in the central cavity of the receptor. This leads to an improper structure of the ligand–receptor complex that may lower the ligand affinity for the receptor. Methylation of a compound possessing quinolinyl moiety seems to enhance the structural/dynamical complementarity between the ligand and the receptor by altering the ligand position. It is worth to notice, that the replacement of the pyrimidine ring by the quinolinyl moiety while piperazine is not methylated (1 → 22) caused a significant decrease (one order of magnitude, approximately) in affinity for the 5-HT<sub>2A</sub> receptor, while the same replacement in case of methylated analogues (15 → 13) induces better structural ligand–receptor adjustment consistent with highly increased affinity of the ligand.

### 3.4. Intrinsic activity

In order to determine postsynaptic 5-HT<sub>1A</sub> receptor agonistic effects of the tested compounds (9–13, 16, 17), their ability to induce lower lip retraction (LLR) in rats and a behavioural syndrome (flat body posture—FBP; and forepaw treading—FT) in reserpinised rats were tested (Tables 3 and 4). The 8-hydroxy-(di-*n*-propylamino)tetralin (8-OH-DPAT)-induced LLR and behavioural syndrome in rats depend on the stimulation of postsynaptic 5-HT<sub>1A</sub> receptors [14,15,55]. Moreover, evidence has been presented that those symptoms are sensitive to 5-HT<sub>1A</sub> receptor antagonists [15,56,57]. Therefore, the ability of the tested compounds to inhibit 8-OH-DPAT-induced LLR, FBP and FT was taken as a measure of 5-HT<sub>1A</sub> receptor (postsynaptic) antagonistic activity (Tables 3 and 4). On the other hand, the 8-OH-DPAT-induced hypothermia in mice is believed to be connected to the activation of presynaptic 5-HT<sub>1A</sub> receptors [58,59] and is abolished by the known 5-HT<sub>1A</sub> antagonists [56,59]. Thus, hypothermia in mice produced by the investigated compounds (and reduced by (S)-WAY 100135, a known 5-HT<sub>1A</sub> receptor antagonist) was regarded as a measure of presynaptic 5-HT<sub>1A</sub> agonistic activity (Tables 5 and 6). Similarly, the ability of the compounds to reverse 8-OH-DPAT-induced hypothermia was taken as a measure of presynaptic antagonistic activity (Table 7).

Table 4  
The induction of serotonin syndrome by compounds **9–12**, **16** and **17** (A) and their effect on the 8-OH-DPAT (5 mg/kg)-induced syndrome (B) in reserpinised rats

Compound	Dose (mg/kg)	Mean $\pm$ SEM			
		A		B	
		Flat body posture	Forepaw treading	Flat body posture	Forepaw treading
Vehicle		0	0	15.0 $\pm$ 0**	13.2 $\pm$ 0.9**
<b>(S)-WAY 100135</b>	2.5	0	0	12.5 $\pm$ 0.7	6.8 $\pm$ 0.7
	5	0	0	9.0 $\pm$ 1.0 # #	5.5 $\pm$ 0.6 # #
	10	0	0	9.7 $\pm$ 1.0 # #	1.0 $\pm$ 0.3 # #
Vehicle		0	0	14.8 $\pm$ 0.2**	13.0 $\pm$ 0.6**
<b>9</b>	10	1.7 $\pm$ 0.4	0	11.8 $\pm$ 0.6 #	10.5 $\pm$ 0.8 #
	20	1.5 $\pm$ 1.3	0	12.3 $\pm$ 0.7 #	9.3 $\pm$ 1.1 # #
Vehicle		0	0	14.8 $\pm$ 0.2**	13.3 $\pm$ 0.4**
<b>10</b>	10	0	0	12.0 $\pm$ 0.9	9.2 $\pm$ 0.7 #
	20	8.5 $\pm$ 1.2*	2.8 $\pm$ 0.6	9.2 $\pm$ 0.1 #	6.8 $\pm$ 0.7 #
Vehicle		0	0	14.8 $\pm$ 0.2**	13.3 $\pm$ 0.4**
<b>11</b>	10	3.8 $\pm$ 1.1*	0.2 $\pm$ 0.2	10.8 $\pm$ 0.9 #	8.7 $\pm$ 1.0 # #
	20	12.8 $\pm$ 0.3**	7.2 $\pm$ 0.7**	8.3 $\pm$ 1.6 # #	9.0 $\pm$ 0.7 # #
Vehicle		0	0	13.8 $\pm$ 0.9**	13.6 $\pm$ 0.5**
<b>12</b>	10	0	0.6 $\pm$ 0.4	9.4 $\pm$ 1.4 # #	9.4 $\pm$ 0.3 # #
	20	10.8 $\pm$ 0.6*	1.5 $\pm$ 0.6	10.8 $\pm$ 0.8 #	6.8 $\pm$ 0.6 # #
Vehicle		0	0	12.7 $\pm$ 0.7**	13.2 $\pm$ 0.8**
<b>13</b>	5	0	0	13.2 $\pm$ 0.6	12.7 $\pm$ 0.7
	10	1.3 $\pm$ 0.6	0	12.2 $\pm$ 0.6	10.7 $\pm$ 0.5 #
	20	3.8 $\pm$ 0.7	0	9.5 $\pm$ 0.8 #	7.7 $\pm$ 0.8 #
Vehicle		0	0	13.3 $\pm$ 0.4**	12.2 $\pm$ 1.3**
<b>16</b>	10	1.7 $\pm$ 0.7	0	8.7 $\pm$ 1.0 # #	7.5 $\pm$ 0.5 # #
	20	6.8 $\pm$ 0.6*	0	7.8 $\pm$ 0.5 # #	4.3 $\pm$ 0.8 # #
Vehicle		0	0	12.2 $\pm$ 0.6**	13.2 $\pm$ 0.8**
<b>17</b>	5	0	0	12.1 $\pm$ 0.7	11.2 $\pm$ 0.9
	10	1.3 $\pm$ 0.6	0	10.1 $\pm$ 1.1	9.0 $\pm$ 1.5
	20	3.3 $\pm$ 1.0	0	11.2 $\pm$ 0.8	6.8 $\pm$ 1.5 #

\*,  $P < 0.05$ ; \*\*,  $P < 0.01$  versus vehicle; #,  $P < 0.05$ ; # #,  $P < 0.01$  versus 8-OH-DPAT.

In behavioural experiments, compounds **10–13**, **16** and **17** (with a differentiated imide fragment) behaved like postsynaptic partial agonists, although their functional profile in used models was not identical. Compounds **11**, **12**, **13** and **17** given alone at doses of 10–20 mg/kg evoked LLR in rats. Moreover, compounds **10**, **11**, **12** and **16** induced some symptoms of behavioural syndrome in reserpine pretreated rats. On the other hand, compounds **10**, **11** and **12** partly inhibited LLR induced by 8-OH-DPAT and, like **13**, **16** and **17**, they reduced behavioural syndrome evoked by that 5-HT<sub>1A</sub> agonist. The functional activity of compounds **11**, **13** and **17** in used models resembles the activity profile described for 5-HT<sub>1A</sub> partial agonists; the behavioural profile of compounds **13** and **17** seems to be approximate to that of ipsapirone, which given alone induced LLR, but not a behavioural syndrome, and inhibited 8-OH-DPAT-induced FBP and FT [55,60–62]. It should, however, be noted that the behavioural effects evoked by these compounds appeared in doses higher than those observed for buspirone or its analogues. Unexpectedly, compound **9** with the same volume of

imide fragment as compound **13** was practically inactive in those behavioural tests.

Out of the compounds tested in vivo, compounds **9**, **10**, **11**, **13** and **16** decreased mice body temperature (Table 5). However, hypothermia induced by compounds **9**, **10**, **11** and **13** (in contrast to compound **16**) was not abolished by (*S*)-WAY 100135; moreover, a decrease of mice body temperature induced by compounds **10** and **13** was enhanced by (*S*)-WAY 100135 (Table 6). Compounds **10** (in lower dose), **12** and **17**—like (*S*)-WAY 100135—did not change the body temperature in mice; in contrast to (*S*)-WAY 100135 and **17**, compounds **10** and **12** did not abolish the hypothermia induced by 8-OH-DPAT (Table 7). Therefore, it seems that 5-HT<sub>1A</sub> presynaptic activity of the compounds **9**, **10**, **11**, **12** and **13** (but not **16** and **17**) is negligible in that experimental paradigm.

### 3.5. Biochemistry

It is known that systemic administration of the selective 5-HT<sub>1A</sub> receptor agonist 8-OH-DPAT dose-depen-

Table 5  
The effect of compounds **9–12**, **16**, **17** on the body temperature in mice

Compound	Dose (mg/kg)	$\Delta t \pm \text{SEM}$ ( $^{\circ}\text{C}$ ) <sup>a</sup>			
		30 min	60 min	90 min	120 min
Vehicle		$-0.2 \pm 0.1$	$-0.2 \pm 0.1$	$-0.3 \pm 0.1$	$-0.2 \pm 0.1$
<b>(S)-WAY 100135</b>	5	$-0.1 \pm 0.2$	$-0.3 \pm 0.2$	$-0.2 \pm 0.1$	$-0.1 \pm 0.1$
	10	$-0.3 \pm 0.2$	$-0.2 \pm 0.1$	$-0.1 \pm 0.1$	$-0.2 \pm 0.1$
	20	$-0.1 \pm 0.1$	$-0.1 \pm 0.2$	$-0.3 \pm 0.1$	$-0.3 \pm 0.1$
<b>9</b>	10	$-0.9 \pm 0.1^{**}$	$-0.4 \pm 0.4$	$-0.5 \pm 0.1$	$-0.3 \pm 0.1$
	20	$-2.4 \pm 0.1^{**}$	$-0.6 \pm 0.1$	$-0.6 \pm 0.1$	$-0.5 \pm 0.1$
	Vehicle	$0.1 \pm 0.1$	$-0.1 \pm 0.2$	$-0.3 \pm 0.1$	$-0.3 \pm 0.1$
<b>10</b>	10	$-0.2 \pm 0.2$	$-0.2 \pm 0.1$	$-0.1 \pm 0.1$	$-0.1 \pm 0.2$
	20	$-0.9 \pm 0.3^{*}$	$-0.1 \pm 0.1$	$-0.1 \pm 0.2^{*}$	$-0.1 \pm 0.2$
	Vehicle	$-0.2 \pm 0.1$	$-0.1 \pm 0.1$	$-0.3 \pm 0.1$	$-0.3 \pm 0.1$
<b>11</b>	10	$-1.4 \pm 0.4^{*}$	$-0.8 \pm 0.2^{*}$	$-0.8 \pm 0.2$	$-0.4 \pm 0.2$
	20	$-2.4 \pm 0.4^{**}$	$-1.7 \pm 0.3^{**}$	$-1.1 \pm 0.2^{*}$	$-0.8 \pm 0.2$
	Vehicle	$-0.2 \pm 0.1$	$-0.1 \pm 0.2$	$-0.2 \pm 0.2$	$-0.1 \pm 0.1$
<b>12</b>	10	$-0.3 \pm 0.2$	$-0.1 \pm 0.2$	$0.2 \pm 0.1$	$0.3 \pm 0.2$
	20	$-0.2 \pm 0.1$	$0.2 \pm 0.1$	$0.5 \pm 0.2^{*}$	$0.6 \pm 0.2^{*}$
	Vehicle	$0.3 \pm 0.1$	$0.0 \pm 0.1$	$0.1 \pm 0.1$	$0.1 \pm 0.1$
<b>13</b>	5	$-0.1 \pm 0.1$	$-0.4 \pm 0.1$	$-0.1 \pm 0.1$	$0.0 \pm 0.1$
	10	$-0.7 \pm 0.1$	$-0.5 \pm 0.1$	$0.0 \pm 0.2$	$0.4 \pm 0.2$
	20	$-1.2 \pm 0.3^{**}$	$-0.1 \pm 0.1$	$-0.1 \pm 0.2$	$0.0 \pm 0.1$
<b>16</b>	10	$0.2 \pm 0.1$	$-0.1 \pm 0.1$	$-0.2 \pm 0.1$	$-0.1 \pm 0.2$
	20	$-0.1 \pm 0.3$	$0.1 \pm 0.1$	$0.2 \pm 0.2$	$0.2 \pm 0.2$
	Vehicle	$-0.7 \pm 0.2^{*}$	$-0.3 \pm 0.2$	$0.1 \pm 0.2$	$0.4 \pm 0.3$
<b>17</b>	5	$0.0 \pm 0.1$	$0.1 \pm 0.2$	$-0.2 \pm 0.2$	$-0.2 \pm 0.1$
	10	$0.2 \pm 0.2$	$0.1 \pm 0.2$	$0.2 \pm 0.2$	$0.1 \pm 0.2$
	20	$-0.4 \pm 0.1$	$-0.2 \pm 0.2$	$0.2 \pm 0.2$	$0.3 \pm 0.2$
Vehicle		$-0.1 \pm 0.2$	$-0.1 \pm 0.1$	$-0.5 \pm 0.2$	$-0.2 \pm 0.2$

\*,  $P < 0.05$ ; \*\*,  $P < 0.01$  versus respective vehicle group.

<sup>a</sup> Absolute mean initial body temperatures were within a range of  $36.4 \pm 0.3$   $^{\circ}\text{C}$ .

dently reduced 5-HT release in striatal and hippocampal dialysates [63]. It was also shown that 5-HT<sub>1A</sub> receptor agonists decreased the 5-HT turnover in the rat hippocampus [64], cortex, hypothalamus and striatum [16,17]. Therefore, we examined the influence of some compounds on the 5-HT turnover in hippocampus and striatum. 5-HT and 5-hydroxyindoleacetic acid (5-HIAA) contents in the frozen tissue samples were measured by HPLC–EC according to the procedure described elsewhere [16,17].

The influence of compounds **16** (active in the presynaptic activity in vivo test) and **13** (inducing hypothermia not reversed by (S)-WAY 100135) on the brain serotonin turnover (as measured by 5-HIAA–5-HT ratio) was examined in the rat tissue homogenates. Compounds **13** and **16** reduced 5-HT turnover in striatum and hippocampus (Fig. 8), exhibiting thus properties of the 5-HT<sub>1A</sub> presynaptic agonists in this model. In agreement with the known data [17,65], a systemic administration of 8-OH-DPAT resulted in the reduction of the serotonin turnover in striatum and hippocampus (Fig. 8).

Table 6

Influence of (S)-WAY 100135 (10 mg/kg) on the hypothermia induced by compounds **9–11**, **13** and **16**

Compound (dose mg/kg)	$\Delta t \pm \text{SEM}$ ( $^{\circ}\text{C}$ ) <sup>a</sup>
Vehicle+vehicle	$-0.2 \pm 0.1$
Vehicle+ <b>9</b> (10)	$-1.0 \pm 0.1^{*}$
(S)-WAY 100135+ <b>9</b> (10)	$-0.7 \pm 0.2^{**}$
Vehicle+vehicle	$0.1 \pm 0.1$
Vehicle+ <b>10</b> (20)	$-1.2 \pm 0.4^{*}$
(S)-WAY 100135+ <b>10</b> (20)	$-1.8 \pm 0.2^{**}$
Vehicle+vehicle	$-0.3 \pm 0.1$
Vehicle+ <b>11</b> (10)	$-1.4 \pm 0.1^{**}$
(S)-WAY 100135+ <b>11</b> (10)	$-1.7 \pm 0.2^{**}$
Vehicle+vehicle	$0.0 \pm 0.1$
Vehicle+ <b>13</b> (20)	$-0.8 \pm 0.1^{**}$
(S)-WAY 100135+ <b>13</b> (20)	$-1.4 \pm 0.3^{**}$
Vehicle+vehicle	$0.1 \pm 0.1$
Vehicle+ <b>16</b> (20)	$-0.6 \pm 0.1^{*}$
(S)-WAY 100135+ <b>16</b> (20)	$-0.3 \pm 0.2$

\*,  $P < 0.05$ ; \*\*,  $P < 0.01$  versus vehicle+vehicle.

<sup>a</sup> Absolute mean initial body temperatures were within a range of  $36.54 \pm 0.4$   $^{\circ}\text{C}$ .

Table 7  
The influence of compounds **10**, **12** and **17** on the 8-OH-DPAT (5 mg/kg)-induced hypothermia in mice

Compound (dose, mg/kg)	$\Delta t \pm \text{SEM}$ ( $\zeta\text{C}$ ) <sup>a</sup>			
	15 min	30 min	45 min	60 min
Vehicle+vehicle	0.3 ± 0.1	0.2 ± 0.2	0.1 ± 0.1	0.1 ± 0.1
Vehicle+8-OH-DPAT	-1.3 ± 0.3*	-1.6 ± 0.2*	-1.1 ± 0.2*	-1.0 ± 0.3*
(S)-WAY 100135 (5)+8-OH-DPAT	-0.2 ± 0.2**	-0.6 ± 0.5	-0.7 ± 0.4	-0.9 ± 0.3
(S)-WAY100135(10)+8-OH-DPAT	0.2 ± 0.2**	0.0 ± 0.2**	0.3 ± 0.2**	0.1 ± 0.2**
Vehicle+vehicle	0.2 ± 0.1	-0.2 ± 0.1	-0.2 ± 0.1	-0.2 ± 0.1
Vehicle+8-OH-DPAT	-1.6 ± 0.3*	-1.6 ± 0.2*	-1.3 ± 0.2*	-0.9 ± 0.2*
<b>10</b> (10)+8-OH-DPAT	-1.8 ± 0.2*	-1.4 ± 0.2*	-1.1 ± 0.2*	0.8 ± 0.2*
Vehicle+vehicle	0.1 ± 0.1	0.1 ± 0.1	-0.2 ± 0.1	-0.2 ± 0.1
Vehicle+8-OH-DPAT	-1.1 ± 0.2*	-1.4 ± 0.2*	-1.1 ± 0.3*	-0.8 ± 0.3
<b>12</b> (20)+8-OH-DPAT	-1.1 ± 0.3*	-1.2 ± 0.2*	-0.8 ± 0.2	-0.4 ± 0.2
Vehicle+vehicle	0.1 ± 0.1	0.0 ± 0.1	0.1 ± 0.1	0.1 ± 0.1
Vehicle+8-OH-DPAT	-1.0 ± 0.2*	-0.9 ± 0.1*	-0.7 ± 0.2*	-0.5 ± 0.2*
<b>17</b> (10)+8-OH-DPAT	0.3 ± 0.2**	0.2 ± 0.2**	-0.1 ± 0.3	0.0 ± 0.2

\*,  $P < 0.05$  versus vehicle+vehicle; \*\*,  $P < 0.01$  versus vehicle+8-OH-DPAT.

<sup>a</sup> Absolute mean initial body temperatures were within a range of  $36.6 \pm 0.4$  °C.

#### 4. Conclusions

Summing up, our results indicate that trisubstituted piperazine-quinolines (but not piperazine-pyrimidines) exhibited a higher affinity to 5-HT<sub>2A</sub> receptors (with the retention of affinity to 5-HT<sub>1A</sub> receptors) than their respective disubstituted analogues. Trisubstituted piperazine-quinolines also exhibited a much higher affinity both to 5-HT<sub>1A</sub> and 5-HT<sub>2A</sub> receptors than their pyrimidine analogues. This result may be rationalised by molecular modelling of the respective ligand–receptor complexes. The molecular simulations suggest that the presence of the methyl group in the piperazine ring of pyrimidine derivatives (e.g. **14**, **15**) induces strong, improper perturbations in the ligand–receptor complexes giving rise to unfavourable interactions and, in consequence, should lead to worse affinities towards 5-HT<sub>1A</sub> as well as 5-HT<sub>2A</sub> receptors (as compared with unmethylated compounds—buspirone (**1**) and gepirone (**3**), respectively). On the other hand, the presence of the methyl group in quinoline derivatives (c.f. **9**, **10**, **11**, **12**, **13**) induces stabilising ligand–receptor interactions with respect to unmethylated compounds (c.f. **18**, **19**, **20**, mesmar (**21**), kaspar (**22**)). Closer intermolecular contacts in the ligand–receptor complexes are probably related to the nature of interactions (steric, electronic, hydrophobic, etc.) underlying experimentally observed better affinities to both of the receptors. For both receptors, the results of the molecular modelling showed that the position occupied by pyrimidine derivatives was different from that of quinolines in the putative binding site. It was also found that the *trans*-membrane helical domains of 5-HT<sub>1A</sub> and 5-HT<sub>2A</sub> receptors have different topographies of the putative binding sites for buspirone analogues. These differences

between 3-D molecular structures of the binding sites may in principle be used to rationalise different ligand affinities towards 5-HT<sub>1A</sub> and 5-HT<sub>2A</sub> receptors. The present theoretical calculations and the experimental affinity results (Table 1) further support the hypothesis [22,23], that the interactions of the active analogues should involve amino acids from TMHs 2, 3, 5, 6 and 7 (as in the **13**-5-HT<sub>1A</sub>, **15**-5-HT<sub>1A</sub> and **13**-5-HT<sub>2A</sub> receptor complexes) but should not involve residues not from TMH1 and the N-terminus (as in the **15**-5-HT<sub>2A</sub> receptor complex; Table 2). The calculations also suggest that compound **13** interacted with 5-HT<sub>1A</sub> receptor in a way characteristic for the receptor activation (in agreement with the functional activity *in vitro* data).

The obtained results of functional study indicate that our trisubstituted piperazines containing quinolinyl (**10**, **11**, **12**, **13**, **16**) or pyrimidinyl (**17**) moiety and differentiated amide fragment exhibited *in vivo* properties of

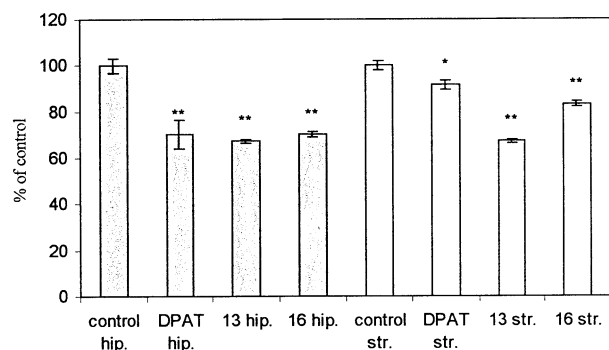


Fig. 8. Effect of 8-OHDPAT (5 mg/kg, i.p.), **13** and **16** (30 mg/kg i.p.) on serotonin turnover in hippocampus (hip.) and striatum (str.). Results are mean  $\pm$  SEM of data obtained from five animals per group; \*,  $P < 0.05$ ; \*\*,  $P < 0.01$ ; the serotonin turnover control values were: hippocampus— $0.848 \pm 0.011$ ; striatum— $0.894 \pm 0.017$ .  $P = 48$ .

the postsynaptic 5-HT<sub>1A</sub> partial agonists. Therefore, it seems that used structural modifications did not diversify their postsynaptic 5-HT<sub>1A</sub> activity. On the other hand, only piperazine-quinoline derivatives with bulky amide part **13** and **16** exhibited features of 5-HT<sub>1A</sub> presynaptic agonists in in vitro test, and compound **16** also in in vivo tests. It should, however, be noted that compound **9**, containing imide part with the same van der Waals volume as **13**, was practically inactive in used models. Interestingly, pyrimidinyl analogue of **16**, compound **17** can be classified as an antagonist of presynaptic 5-HT<sub>1A</sub> receptors.

## References

- [1] L.E. Schechter, P. McGonigle, J.E. Barrett, Serotonergic antidepressants: current and future perspectives, *Curr. Opin. CPNS Invest. Drugs* 1 (1999) 432–447.
- [2] L.R. Levine, W.Z. Potter, 5-HT<sub>1A</sub> agonists, partial agonists and antagonists in anxiety and depression: a lost cause, *Curr. Opin. CPNS Invest. Drugs* 1 (1999) 448–452.
- [3] P.C. Moser, M.D. Tricklebank, D.N. Middlemiss, A.K. Mir, M.F. Hibert, J.R. Fozard, Characterization of MDL 73005EF as a 5-HT<sub>1A</sub> selective ligand and its effects in animal models of anxiety: comparison with buspirone, 8-OH-DPAT and diazepam, *Br. J. Pharmacol.* 99 (1990) 343–349.
- [4] J. DeVry, 5-HT<sub>1A</sub> receptor agonists: recent developments and controversial issues, *Psychopharmacology* 121 (1995) 1–26.
- [5] Drug status update, *Curr. Res. Serotonin* 3 (1998) 164–173.
- [6] J.E. Barrett, L. Zhang, Anticonflict and discriminative stimulus effects of the 5-HT<sub>1A</sub> compounds WY-47,846 and WY-48,723 and the mixed 5-HT<sub>2</sub> agonist/5-HT<sub>2</sub> antagonist WY-50,324 in pigeons, *Drug Dev. Res.* 24 (1991) 179–188.
- [7] A. Sing, J. Lucki, Antidepressant-like activity of compounds with varying efficacy at 5-HT<sub>1A</sub> receptors, *Neuropharmacology* 32 (1993) 331–340.
- [8] C. Darlington, Flibanserin, *CPNS Invest. Drugs* 1 (1999) 510–513.
- [9] M. Cybulski, Z. Chilmonczyk, Synthesis of 1,2,4-substituted piperazines, new 5-HT<sub>1A</sub> receptor ligands, *Acta Pol. Pharm. Drug Res.* 58 (2001) 357–365.
- [10] Z. Chilmonczyk, A. Leś, A. Woźniakowska, J. Cybulski, A.E. Koziol, M. Gdaniec, Buspirone analogues as ligands of the 5-HT<sub>1A</sub> receptor. 1. The molecular structure of buspirone and its two analogues, *J. Med. Chem.* 38 (1995) 1701–1710.
- [11] Z. Chilmonczyk, A. Szelejewska-Woźniakowska, J. Cybulski, M. Cybulski, A.E. Koziol, M. Gdaniec, Conformational flexibility of serotonin<sub>1A</sub> receptor ligands from crystallographic data. Updated model of the receptor pharmacophore, *Arch. Pharm. Pharm. Med. Chem.* 330 (1997) 146–160.
- [12] D.N. Middlemiss, J.R. Fozard, 8-Hydroxy-2-(di-*n*-propylamino)-tetralin discriminates between subtypes of the 5-HT<sub>1</sub> recognition site, *Eur. J. Pharmacol.* 9 (1983) 151–153.
- [13] A.J. Bojarski, M.T. Cegła, S. Charakchieva-Minol, M.J. Mokrosz, M. Maćkowiak, S. Misztal, J.L. Mokrosz, Structure–activity relationship studies of CNS agents. Part 9. 5-HT<sub>1A</sub> and 5-HT<sub>2</sub> receptor affinity of some 2- and 3-substituted 1,2,3,4-tetrahydro-carbolines, *Pharmazie* 48 (1993) 289–294.
- [14] H.H.G. Berendsen, F. Jenck, C.L.E. Broekkamp, Selective activation of 5-HT<sub>1A</sub> receptors induces lower lip retraction in rats, *Psychopharmacology* 101 (1990) 57–61.
- [15] M.B. Tricklebank, C. Forler, J.R. Fozard, The involvement of subtypes of the 5-HT<sub>1A</sub> receptor and of catecholaminergic systems in the behavioural response to 8-hydroxy-2-(di-*n*-propylamino)tetralin in the rat, *Eur. J. Pharmacol.* 106 (1984) 271–282.
- [16] K. Gołombiowska, Ipsapirone, a new anxiolytic drug, stimulates catecholamine turnover in various regions of the rat brain, *Pol. J. Pharmacol. Pharm.* 42 (1990) 143–150.
- [17] K. Gołombiowska, Effect of acute and chronic treatment of rats with the putative anxiolytic drug ipsapirone on the turnover of monoamine transmitters in various brain regions. A comparison with the 5-HT<sub>1A</sub> agonist 8-OH-DPAT, *Pol. J. Pharmacol. Pharm.* 44 (1992) 15–24.
- [18] T.E. Ferrin, The MIDAS display system, *J. Mol. Graphics* 6 (1988) 13–27.
- [19] W.D. Cornell, P. Cieplak, C.I. Bayly, P.A. Kollman, Application of RESP charges to calculate conformational energies, hydrogen bond energies and free energies of solvation, *J. Am. Chem. Soc.* 115 (1993) 9620–9631.
- [20] M.J. Frisch, G.W. Trucks, H.B. Schlegel, P.M.W. Gill, B.G. Johnson, M.A. Robb, J.R. Cheeseman, T. Keith, G.A. Petersson, J.A. Montgomery, K. Raghavachari, M.A. Al-Laham, V.G. Zakrzewski, J.V. Ortiz, J.B. Foresman, J. Cioslowski, B.B. Stefanov, A. Nanayakkara, M. Challacombe, C.Y. Peng, P.Y. Ayala, W. Chen, M.W. Wong, J.L. Andres, E.S. Replogle, R. Gomperts, R.L. Martin, D.J. Fox, J.S. Binkley, D.J. Defrees, J. Baker, J.P. Stewart, M. Head-Gordon, C. Gonzalez, J.A. Pople, GAUSSIAN 94, Revision D.1. Gaussian, Inc., Pittsburgh, PA, 1995.
- [21] D.A. Case, D.A. Pearlman, J.W. Caldwell, T.E. Cheatham III, W.S. Ross, C. Simmerling, T. Darden, K.M. Merz, R.V. Stanton, A. Cheng, J.J. Vincent, M. Crowley, D.M. Ferguson, R. Radmer, G.L. Seibel, U. Chandra Singh, P. Weiner, P.A. Kollman, AMBER 5. UCSF, San Francisco, 1997.
- [22] A. Bronowska, A. Leś, Z. Chilmonczyk, S. Filipek, O. Edvardsen, R. Ostensen, I. Sylte, Molecular dynamics of buspirone analogues interacting with the 5-HT<sub>1A</sub> and 5-HT<sub>2A</sub> receptors, *Bioorg. Med. Chem.* 9 (2001) 881–895.
- [23] A. Bronowska, Z. Chilmonczyk, A. Leś, S. Filipek, O. Edvardsen, R. Ostensen, I. Sylte, Molecular dynamics of 5-HT<sub>1A</sub> and 5-HT<sub>2A</sub> serotonin receptors with methylated buspirone analogues, *J. Comp. Aid. Mol. Des.* (2001), in press.
- [24] H. Nakamura, T. Sakamoto, A. Wada, A theoretical study of the dielectric constant of protein, *Protein Eng.* 2 (1988) 177–183.
- [25] A. Bronowska, Molecular modelling of interactions between serotonin receptors and their ligands, Doctoral dissertation, University of Warsaw, Warsaw, 2001.
- [26] P.A. Chanda, M.C.W. Michin, A.R. Davis, L. Greenberg, Y. Reilly, W.H. McGregor, R. Bhat, M.H. Lubeck, S. Mizutani, P.P. Hung, Identification of residues important for ligand binding to the human 5-hydroxytryptamine<sub>1A</sub> serotonin receptor, *Mol. Pharmacol.* 43 (1993) 516–520.
- [27] I. Sylte, Z. Chilmonczyk, S.G. Dahl, J. Cybulski, Ø. Edvardsen, The ligand binding site of buspirone analogs at the 5-HT<sub>1A</sub> receptor, *J. Pharm. Pharmacol.* 49 (1997) 698–705.
- [28] K. Palczewski, T. Kumasaka, T. Hori, C.A. Behnke, H. Motoshima, B.A. Fox, I. Le Trong, D.C. Teller, T. Okada, R.E. Stenkamp, M. Yamamoto, M. Miyano, Crystal structure of rhodopsin: a G protein-coupled receptor, *Science* 289 (2000) 739–745.
- [29] G.F.X. Schertler, C. Villa, R. Henderson, Projection structure of rhodopsin, *Nature* 362 (1993) 770–772.
- [30] V.M. Unger, G.F.X. Schertler, Low resolution structure of bovine rhodopsin determined by electron cryo-microscopy, *Biophys. J.* 68 (1995) 1776–1786.
- [31] J.M. Baldwin, The probable arrangement of the helices in G protein-coupled receptors, *EMBO J.* 12 (1993) 1693–1703.
- [32] J.M. Baldwin, G.F.X. Schertler, V.M. Unger, An  $\alpha$ -carbon template for the transmembrane helices in the rhodopsin family

- of G-protein coupled receptors, *J. Mol. Biol.* 272 (1997) 144–164.
- [33] E.H. Cook Jr., K.E. Fletcher, M. Wainwright, N. Marks, S.Y. Yan, B.L. Leventhal, Primary structure of the human platelet serotonin 5-HT<sub>2A</sub> receptor: identify with frontal cortex serotonin 5-HT<sub>2A</sub> receptor, *J. Neurochem.* 63 (1994) 465–469.
- [34] D.A. Pearlman, D.A. Case, J.W. Caldwell, W.S. Ross, T.E. Cheatham III, S. DeBolt, D.M. Ferguson, G.L. Seibel, P.A. Kollman, *Comp. Phys. Commun.* 91 (1995) 1–41.
- [35] D.L. Farrens, C. Altenbach, K. Yang, W.L. Hubbel, H.G. Khorana, Requirement of rigid body motion of transmembrane helices for light activation of rhodopsin, *Science* 274 (1996) 768–770.
- [36] J. Liu, N. Blin, B.R. Conklin, J. Wess, Molecular mechanisms involved in muscarinic acetylcholine receptor-mediated G protein activation studied by insertion mutagenesis, *J. Biol. Chem.* 271 (1996) 6172–6178.
- [37] I. Sylte, A. Bronowska, S.G. Dahl, *Eur. J. Pharmacol.* 416 (2001) 33.
- [38] F. Fanelli, C.M. Menziani, A. Scheer, S. Cotecchia, P.G. De Benedetti, Ab initio modeling and molecular dynamics simulation of the alpha 1b-adrenergic receptor activation, *Methods* 14 (1998) 302–317.
- [39] B.Y. Ho, A. Karschin, T. Branchek, N. Davidson, H.A. Lester, The role of conserved aspartate and serine residues in ligand binding and in function of the 5-HT<sub>1A</sub> receptor: a site-directed mutagenesis study, *FEBS Lett.* 312 (1992) 259–263.
- [40] X.-M. Guan, S.J. Peroutka, B.K. Kobilka, Identification of a single amino acid residue responsible for the binding of a class of  $\beta$ -adrenergic receptor antagonists to the 5-hydroxytryptamine<sub>1A</sub> receptors, *Mol. Pharmacol.* 41 (1992) 695–698.
- [41] B.L. Roth, M. Shokam, M.S. Choudhary, N. Khan, Identification of conserved aromatic residues essential for agonist binding and second messenger production at 5-hydroxytryptamine<sub>2A</sub> receptors, *Mol. Pharmacol.* 52 (1997) 259–266.
- [42] J. Lappalainen, L. Zhang, M. Dean, M. Oz, N. Ozaki, D.H. Yu, M. Virkkunen, F. Wieght, M. Linnoila, D. Goldman, Identification, expression, and pharmacology of a Cys23–Ser23 substitution in the human 5-HT<sub>2C</sub> receptor gene (HTR2C), *Genomics* 27 (1995) 274–279.
- [43] K. Ling, P. Wang, J. Zhao, Y.L. Wu, Z.J. Cheng, G.X. Wu, W. Hu, L. Ma, G. Pei, Five-transmembrane domains appear sufficient for a G-protein coupled receptor: functional five-transmembrane domain chemokine receptors, *Proc. Natl. Acad. Sci. USA* 96 (1999) 7927–7929.
- [44] W. Zhou, C. Flanagan, J.A. Ballesteros, K. Konvicka, J.S. Davidson, H. Weinstein, R.P. Millar, S.C. Sealfon, A reciprocal mutation supports helix 2 and helix 7 proximity in the gonadotropin-releasing hormone receptor, *Mol. Pharmacol.* 45 (1994) 165–170.
- [45] E.A. Zhukovsky, P.R. Robinson, D.D. Oprian, Transducin activation by rhodopsin without a covalent bond to the 11-*cis*-retinal chromophore, *Science* 251 (1991) 558–560.
- [46] K. Wieland, H.M. Zuurmond, C. Krasel, A.P. Ijerman, M.J. Lohse, Involvement of Asn-293 in stereospecific agonist recognition and in activation of the  $\beta$ 2-adrenergic receptor, *Proc. Natl. Acad. Sci. USA* 93 (1996) 9276–9281.
- [47] U. Gether, S. Lin, P. Ghanouni, J.A. Ballesteros, H. Weinstein, B.K. Kobilka, Agonists induce conformational changes in transmembrane domains III and VI of the  $\beta$ 2 adrenoreceptors, *EMBO J.* 16 (1997) 6737–6747.
- [48] H.R. Bourne, How receptors talk to trimeric G protein, *Curr. Opin. Cell Biol.* 9 (1997) 134–142.
- [49] J. Liu, B.R. Conklin, N. Blin, J. Yun, J. Wess, Identification of a receptor/G-protein contact site critical for signalling specificity and G-protein activation, *Proc. Natl. Acad. Sci. USA* 92 (1995) 11642–11646.
- [50] S.C. Sealfon, L. Chi, B.J. Ebersole, V. Rodic, D. Zhang, J.A. Ballesteros, H. Weinstein, Related contribution of specific helix 2 and 7 residues to conformational activation of the serotonin 5-HT<sub>2A</sub> receptor, *J. Biol. Chem.* 270 (1995) 16683–16688.
- [51] F. Buck, W. Meyerhof, H. Werr, D. Richter, Characterization of N- and C-terminal deletion mutants of the rat serotonin HT<sub>2</sub> receptor in *Xenopus laevis* oocytes, *Biochem. Biophys. Res. Commun.* 178 (1991) 1421–1428.
- [52] M.G. Eason, S.B. Liggett, Identification of Gs coupling domain in the amino acid terminus of the third intracellular loop of the  $\alpha$ 2A-adrenergic receptor. Evidence for distinct structural determinants that confer Gs versus Gi coupling, *J. Biol. Chem.* 270 (1995) 24753–24760.
- [53] N. Almaula, B.J. Ebersole, D. Zhang, H. Weinstein, S.C. Sealfon, Mapping the binding site pocket of the serotonin 5-hydroxytryptamine<sub>2A</sub> receptor. Ser3.36(159) provides a second interaction site for the protonated amine of serotonin but not of lysergic acid diethylamide or bufotenin, *J. Biol. Chem.* 271 (1996) 14672–14675.
- [54] H.T. Kao, N. Adham, M.A. Olsen, R.L. Weinshank, T.A. Branchek, P.R. Hartig, Site-directed mutagenesis of a single residue changes the binding properties of the serotonin 5-HT<sub>2</sub> receptor from a human to a rat pharmacology, *FEBS Lett.* 307 (1992) 324–328.
- [55] H.H.G. Berendsen, C.L.E. Broekkamp, A.M.L. Van Delft, Depletion of brain serotonin differently affects behaviors induced by 5-HT<sub>1A</sub>, 5-HT<sub>1C</sub> and 5-HT<sub>2</sub> receptor activation, *Behav. Neural Biol.* 55L (1991) 214–226.
- [56] E. Przegaliński, M. Filip, B. Budziszewska, E. Chojnacka-Wójcik, Antagonism of (+)-WAY 100135 to behavioural, hypothermic and corticosterone effects induced by 8-OH-DPAT, *Pol. J. Pharmacol.* 46 (1994) 21–27.
- [57] J.L. Mokrosz, M.H. Paluchowska, E. Chojnacka-Wójcik, M. Filip, S. Charakchieva-Minol, A. Dereń-Wesołek, M.J. Mokrosz, Structure–activity relationship studies of central nervous system agents. 13. 4-[3-(Benzotriazol-1-yl)propyl]-1-(2-methoxyphenyl)piperazine, a new putative 5-HT<sub>1A</sub> receptor antagonist, and its analogues, *J. Med. Chem.* 37 (1994) 2754–2760.
- [58] G.M. Goodwin, R.J. De Souza, A.R. Green, The pharmacology of the hypothermic response in mice response to 8-hydroxy-2-(di-*n*-propylamino)tetralin (8-OH DPAT), *Neuropharmacology* 24 (1985) 1187–1194.
- [59] K.F. Martin, D.J. Heal, 8-OH-DPAT-induced hypothermia in rodents: a specific model of 5-HT<sub>1A</sub> autoreceptor function, in: J.R. Fozard, P.R. Saxena (Eds.), *Serotonin: Molecular Biology, Receptors and Functional Effects*, Birkhauser Verlag, Basel, 1991, pp. 483–490.
- [60] J.L. Mokrosz, A. Dereń-Wesołek, E. Tatarczyńska, B. Duszyńska, A.J. Bojarski, M.J. Mokrosz, E. Chojnacka-Wójcik, 8-[4-[2-(1,2,3,4-Tetrahydroisoquinolinyl)]-butyl]-8-azaspiro[4.5]dekan-7,9-dione: a new 5-HT<sub>1A</sub> receptor ligand with the same activity profile as buspirone, *J. Med. Chem.* 39 (1996) 1125–1129.
- [61] L.M. Smith, S.J. Peroutka, Differential effects 5-hydroxytryptamine selective drugs on the 5-HT behavioral syndrome, *Pharmacol. Biochem. Behav.* 24 (1986) 1513–1519.
- [62] J. Maj, E. Chojnacka-Wójcik, E. Tatarczyńska, A. Kłodzińska, Central action of ipsapirone, a new anxiolytic drug, on serotonergic, noradrenergic and dopaminergic function, *J. Neural Transm.* 7 (1997) 1–70.
- [63] D.S. Kreiss, I. Lucki, Differential regulation of serotonin (5-HT) release in the striatum and hippocampus by 5-HT<sub>1A</sub> autoreceptors of the dorsal and median raphé nuclei, *J. Pharmacol. Exp. Ther.* 269 (1994) 1268–1279.



- [64] H.Y. Ye Liu, H.B. Li, A.R. Martin, U. Hacsell, T. Lewander, Pharmacodynamic and pharmacokinetic studies in rats of *S*-8-(2-furyl)- and *R*-8-phenyl-2-(di-*n*-propylamino)-tetalin, two novel 5-HT<sub>1A</sub> receptor agonists in vitro with different properties in vivo, *J. Pharm. Pharmacol.* 49 (1997) 169–177.
- [65] S. Hjorth, A. Carlson, T. Magnusson, L.E. Arvidson, In vivo biochemical characterization of 8-OH-DPAT: evidence for 5-HT receptor selectivity and agonist action in rat CNS, in: C.T. Durish, S. Ahlenius, P.H. Hutson (Eds.), *Brain 5-HT<sub>1A</sub> Receptors*, Wiley, Chichester, 1987, pp. 94–105.
- [66] J.L. Mokrosz, P. Pietrasiewicz, B. Duszyńska, T.M. Cegła, Structure–activity relationship studies of central nervous system agents. 5. Effect of the hydrocarbon chain on the affinity of 4-substituted 1-(3-chlorophenyl)piperazines for 5-HT<sub>1A</sub> receptor site, *J. Med. Chem.* 35 (1992) 2369–2374.
- [67] D. Hoyer, Functional correlates of serotonin 5-HT<sub>1</sub> recognition site, *J. Rec. Res.* 8 (1988) 59–81.
- [68] E. Zifa, G. Fillion, 5-Hydroxytryptamine receptors, *Pharm. Rev.* 44 (1992) 402–458.